International Journal of Modern Physics C
Vol. 34, No. 11 (2023) 2350153 (14 pages)

DOI: 10.1142/S012918312350153X

World Scientific
www.worldscientific.com

Electron–lattice pair properties in chains with cubic interaction

M. S. S. Junior*, M. O. Sales† and F. A. B. F. de Moura*,‡

*Instituto de Física, Universidade Federal de Alagoas, Maceió, Alagoas 57072-970, Brazil

†IFMA Campus São João dos Patos, Rua Padre Santiago, s/n, Centro, São João dos Patos, Maranhão 65665-000, Brazil

‡fidelis@fis.ufal.br

Received 5 July 2022
Accepted 31 March 2023
Published 6 May 2023

In this paper, we investigate the one-electron propagation in a nonlinear chain with electron–lattice interaction. The model contains standard cubic nonlinear terms, and we introduce the coupling between the electron and the lattice through the hopping distribution. We solve the coupled equation set to electron and lattice and calculate the electronic position as a function of time. We provide a detailed investigation of the electron and lattice dynamics for a wide range of electron–lattice coupling intensities. Our results demonstrate that depending on the initial condition we consider and the intensity of the electron–lattice interaction, we can obtain (or not) an electron–phonon pair formation. Our results reveal that, depending on the initial velocity of the lattice and the degree of electron–lattice term, we can observe a repulsion between electron and lattice deformations.

Keywords: Localization; electron–lattice; nonlinear.

1. Introduction

The electronic-phonon phenomenology attracted a great attention in the last years.[1–34] Within the context of one electron in a one-dimensional tight-binding Hamiltonian, one of the most relevant contributions was the Su, Schrieffer and Heeger (SSH) model.[8] Within the SSH framework, off-diagonal terms are directed dependents on the lattice vibrations. By using an atom-optics setup, an experimental quantum simulation of this model was provided.[9]

Other interesting works were done by Davydov.[35–39] The Davydov formalism describes the interaction of exciton modes related to the amide-I excitation with

‡Corresponding author.

the lattice phonons. It was pointed out that the possibility of the electron–lattice coupling provides electronic propagation. Within the context of nonlinear lattices, a wide collection of works had been showed in the past.[31,40–54] Velarde pointed out the possibility of electronic transport mediated by solectrons (a "quasi-particle" originated from the coupling between self-trapped states and nonlinear solitons). Based on this theory, the electronic transport mediated by this electron–soliton phenomenology has been investigated in several two-dimensional anharmonic lattices, particularly in a square lattice similar to the "cuprate" lattice.[50]

In Ref. 55, an experimental study of tunneling dynamics was carried out on a sub-nanosecond time scale. Surface acoustic waves (SAWs) were used to generate dynamic quantum dots in a one-dimensional channel, in which these dots transport one electron each at SAW velocity. In Ref. 56, the time evolution of a single electron wave function was studied using moving quantum dots defined by SAW. As the bandwidth limits the coherent dynamics of the system, a procedure was proposed to overcome this. Quantum dots travel through a static potential and different confinement regions, causing electrons to be excited in a superposition of state. It was investigated experimentally by electron transport correlated with the aid of a SAW in almost one-dimensional channels.[57] These electrons were transported through three micron-separated channels formed in a heterostructure. The SAW traps electrons and leads them into two depleted channels connected to an open ballistic channel. In Ref. 58, it was demonstrated experimentally using a source and detector of a single electron propagating in isolation from the other electrons in a one-dimensional channel. This channel was placed between two quantum dots, and a SAW transported this electron through the channel with a velocity 3 μm ns^{-1}. The emission and reception efficiencies are 96% and 92%, respectively. In Ref. 59, the authors move a single electron along a channel using a SAW. In Ref. 60, the authors perform an exciting experiment in graphene under a SAWs effect on a piezoelectric surface. They demonstrate the existence of an acoustoelectric current crossing the graphene structure. In Ref. 61, it was experimentally demonstrated that in semiconductor heterostructures such as GaAs/AlGaAs, the electronic propagation between distant quantum dots can be obtained using SAW. They obtain a single-shot transfer with an efficiency of 99%. In Ref. 62, an experimental study was carried out for the generation of single photons, without using quantum dots. They transported a single electron at a minimum potential of a SAW to a region of holes to form an exciton. In Ref. 63, the dynamics of electrons between two coupled wires under the effect of SAW was investigated in detail. They prove that coherent tunneling occurs when the electrostatic potential generated by the SAW is specially aligned between the two coupled wires. In Ref. 64, an experimental analysis of a SAW waveguide in lithium niobate ($LiNbO_3$) was carried out from a line defect within a triangular photonic lattice. The SAW mode involves extensive bandwidth and demonstrates isolation in the lateral direction in such a waveguide.

In this work, we describe the electron–lattice pair formation in models with cubic nonlinearity. The problem of a one electron moving in a Fermi–Pasta–Ulam

chain was investigated in the past[53] however, a more detailed description of the possibility of electron–soliton propagation was not done. Here we investigate the occurrence of the electron–lattice pair and its dependence on the initial condition and the electron–phonon interaction. Our results demonstrate the optimal condition to obtain the electronic dynamics controlled by the solitonic propagation. We also investigate the amount of the wave function that the lattice deformation can capture and its dependence on the initial condition and electron–lattice coupling. Our calculations indicate that the occurrence of electron–soliton pairs is a rare phenomenon. The electron wave function and the lattice's deformation remain separated even for intense electron–lattice interaction.

2. Model

We investigate the propagation of a one electron in a chain with N masses. We can write the electronic tight-binding Hamiltonian as follows:

$$H_e = \sum_j V_{j,j+1}(c_{j+1}^{\dagger}c_j + c_j^{\dagger}c_{j+1}), \tag{1}$$

where the operators $c_j^{\dagger}$ and c_j are the creation and annihilation operators for the electron at site j. $V_{j,j+1}$ represents the electron's kinetic energy (the hopping term) that depends on the distance between two consecutive masses. In our model, we have $V_{j,j+1} = -[1 - \alpha(Q_{j+1} - Q_j)]$.[8] The quantity Q_j represents the displacement of the mass at site (j) from its equilibrium position. α is a tunable parameter that determines the electron–lattice coupling strength. The lattice dynamics will be obtained by considering that the chain is a Fermi–Pasta–Ulam chain with N masses with classical Hamiltonian given by[53]

$$H_L = \sum_j \left\{ \frac{P_j^2}{2} + \frac{1}{4}[(Q_{j+1} - Q_j)^2 + (Q_j - Q_{j-1})^2] \right\} + \sum_j \left\{ \frac{1}{6}[(Q_{j+1} - Q_j)^3 + (Q_j - Q_{j-1})^3] \right\}. \tag{2}$$

We emphasize that all masses are equal to unit ($m_j = 1$). P_j represents the momentum the jth mass. The lattice equation can be written as $-\frac{\partial H}{\partial Q_j} = a_j(t)$ where

$$a_j(t) = (Q_{j+1} - Q_j) - (Q_j - Q_{j-1})] + [(Q_{j+1} - Q_j)^2 - (Q_j - Q_{j-1})^2] - \alpha\{(c_{j+1}^{*}c_j + c_{j+1}c_j^{*}) - (c_j^{*}c_{j-1} + c_j c_{j-1}^{*})\}. \tag{3}$$

The time-dependent wave function $|\Phi(t)\rangle = \sum_j c_j(t)|j\rangle$ will be obtained by numerical solution of the time-dependent Schrödinger. We consider the electron initially localized at site $N/2$, i.e. $|\Phi(t=0)\rangle = \sum_j c_j(t=0)|j\rangle$ where $c_j(t=0) = \delta_{j,N/2}$. The Wannier amplitudes evolve in time according to the time-dependent

Schrödinger equation as ($\hbar = 1$)

$$i\frac{dc_j(t)}{dt} = -[1-\alpha(Q_{j+1}-Q_j)]c_{j+1}(t) - [1-\alpha(Q_j-Q_{j-1})]c_{j-1}(t). \quad (4)$$

The classical equation was solved by using a standard Verlet velocity formalism.[65] The position at time Δt is given by $Q_j(t=\Delta t) \approx Q_j(t=0) + P_j(t=0)(\Delta t) + [(\Delta t)^2/2]a_j(t=0)$. The momentum at time Δt is given by $P_j(t=\Delta t) \approx P_j(t=0) + (\Delta t/2)(a_j(t=0) + a_j(t=\Delta t))$. We emphasize that for initial times, the lattice position and velocity were considered such as $Q_j(t=0) = 0$ and $P_j = v_0\delta_{j,N/2}$. In this kind of initial condition, i.e. an initial impulse excitation, we can excite the nonlinear solitonic modes that this cubic model can exhibit.[53] The electron dynamics equations (Eq. (4)) were solved numerically by using a high-order method based on the Taylor expansion[66] of the evolution operator $U(\Delta t) = \exp(-iH_e\Delta t) = 1 + \sum_{l=1}^{n_o} \frac{(-iH_e\Delta t)^l}{l!}$ where H_e is the one-electron Hamiltonian. The wave function at time Δt is given by $|\Phi(\Delta t)\rangle = U(\Delta t)|\Phi(t=0)\rangle$. This combined method (Verlet + Taylor) can be used recursively to obtain the displacement, momentum and the wave function at time t. The following results were taken by using $\Delta t = 2\times10^{-3}$ and $n_o = 10$. Our analysis will be done by following the electron and the lattice deformation propagation along the chain. The electronic propagation can be analyzed by using the quantity n_e defined as follows:

$$n_e = \sum_j (j - N/2)|c_j(t)|^2. \quad (5)$$

We compute the electronic velocity (V_e) by using a linear fitting of the curve $n_e \times t$. The lattice deformation will be analyzed using an effective probability of deformations Π_j defined as follows:

$$\Pi_j = A_j \Big/ \sum_j A_j, \quad (6)$$

where $A_j = (1 - e^{-(Q_j - Q_{j-1})})^2$. The centroid of the deformation wave's (n_L) can be obtained as follows:

$$n_L = \sum_j (j - N/2)\Pi_j. \quad (7)$$

We obtain the propagation velocity of the lattice deformations (V_L) following a similar way as was used for finding V_e (i.e. a linear fitting of the curve $n_L \times t$).

3. Results

We show our results about the electron–lattice dynamics within this cubic nonlinear model. We emphasize that we solve the model considering a chain with $N = 10^5$ sites. However, we have used the self-expanded trick to speed up the calculation. Therefore, we start our calculations in a small fraction of the chain around the center of chain (with size $N_0 = 200$). Whenever the electron wave function (or

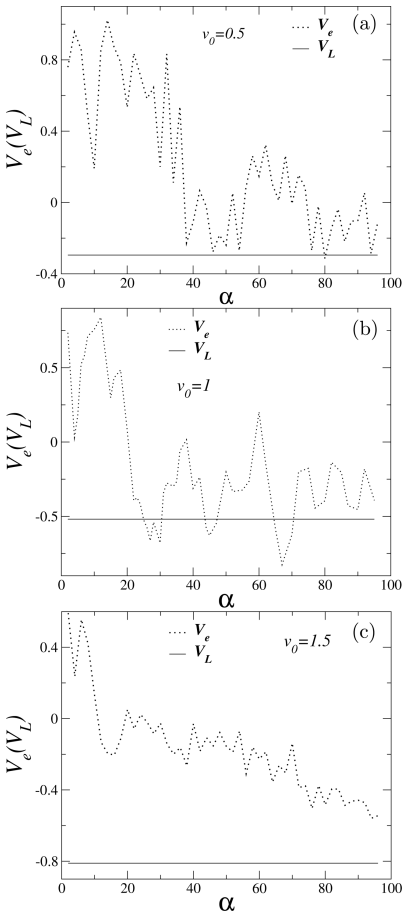

Fig. 1. Velocity of the electron (V_e) and the lattice (V_L) vs the electron–lattice coupling. The initial lattice velocity was $v_0 = -0.5$ upto -1.5.

the lattice vibrations) arrives at the boundary of this segment, we increase the value of N_0. We stress that we consider the electron initially localized at site $N/2$, i.e. $|\Phi(t=0)\rangle = \sum_j c_j(t=0)|j\rangle$ where $c_j(t=0) = \delta_{j,N/2}$. The initial condition considered for the lattice was $Q_j(t=0) = 0$ and $P_j = v_0\delta_{j,N/2}$. In Fig. 1, we plot the velocity of the electron and the lattice vs the electron–lattice coupling. We calculate V_e and V_L following the same procedure: we calculate curves of n_e vs t (and n_L vs t); using these curves, we applied a linear fitting to calculate V_e and V_L, respectively. We emphasize that the curves of n_e and n_L were considered from $t = 0$ upto t_m (with $t_m > 10^4$ time units). The initial lattice velocity was $v_0 = 0.5$ upto 1.5. By analyzing these results, we can see that the lattice deformation kept its velocity roughly independent of the electron–lattice interaction. Moreover, we observe that the magnitude of the lattice's velocity exhibits some dependence on the initial velocity.[54] This phenomenology is directly dependent of the kind of

nonlinearity we have considered in our model.[54] Chains with cubic nonlinearity that were started with initial impulse excitation promote the appearance of a nonlinear stable solitonic mode.[53] This soliton mode travels along the chain with velocity roughly constant (independent of the electron–lattice coupling). Therefore, the solid line obtained in our calculations indicates precisely this solitonic mode's presence. On another side, the dotted line indicates the electronic velocity and its dependence on the electron–lattice interaction. We can see that the electronic dynamics strongly depend on the value of α and the initial lattice velocity. We can see that the electron and the lattice dynamics exhibit distinct velocities for a wide range of values of α and v_0. We observe that a good concordance between V_e and V_L was obtained only for $v_0 = 1$ and some values of α (for α about [24–30], [45–50] and [65–70]). In general, for a wide range of values of α, our calculations indicate that the electron and the lattice solitonic mode travel with distinct velocities. In Fig. 2, we plot the

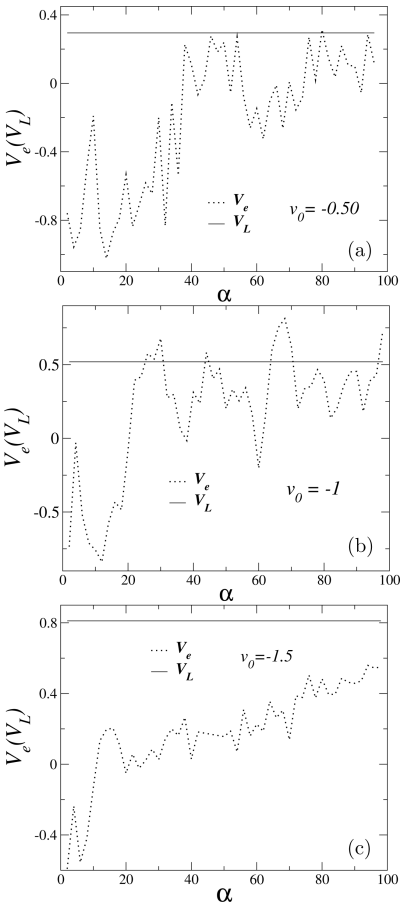

Fig. 2. Velocity of the electron (V_e) and the lattice (V_L) vs the electron–lattice coupling. The initial lattice velocity was $v_0 = -0.5$ upto -1.5.

same results as in Fig. 1 considering the initial lattice velocity with same values as in Fig. 1 however with opposite signal. The results in Fig. 2 are qualitatively similar to those shown in Fig. 1. For a wide range of values of α, we can see that the electron wave function and the lattice's vibrations remain roughly separated. For some specifics ranges of α, we observe that V_e and V_L have relative values (thus suggesting that both excitation are close). We also observe in Fig. 2 that the signal of velocities V_e and V_L is inverted in comparison with those results in Fig. 1. It is a direct consequence of the initial velocity v_0 we consider.[54] The solitonic excitation's velocity depends on the initial impulse's magnitude and signal.

In Figs. 3 and 4, we show the normalized distance between the electron and the lattice's deformation $D_{e,L}/D_m$. We emphasize that $D_{e,L} = |n_e(t) - n_L(t)|_{t \approx t_m}$ (with $t_m > 10^4$ time units). The quantity D_m represents the maximum value of $D_{e,L}$. In good agreement with the previous results shown in Figs. 1 and 2, the electron and the lattice's deformations remain separated for a wide range of values of α. For regions where V_e and V_L are close, we obtain a small (almost zero) normalized distance $D_{e,L}/D_m$. We also observe that, qualitatively, these results are roughly the same, independent of the signal and magnitude of the initial velocity v_0. Our

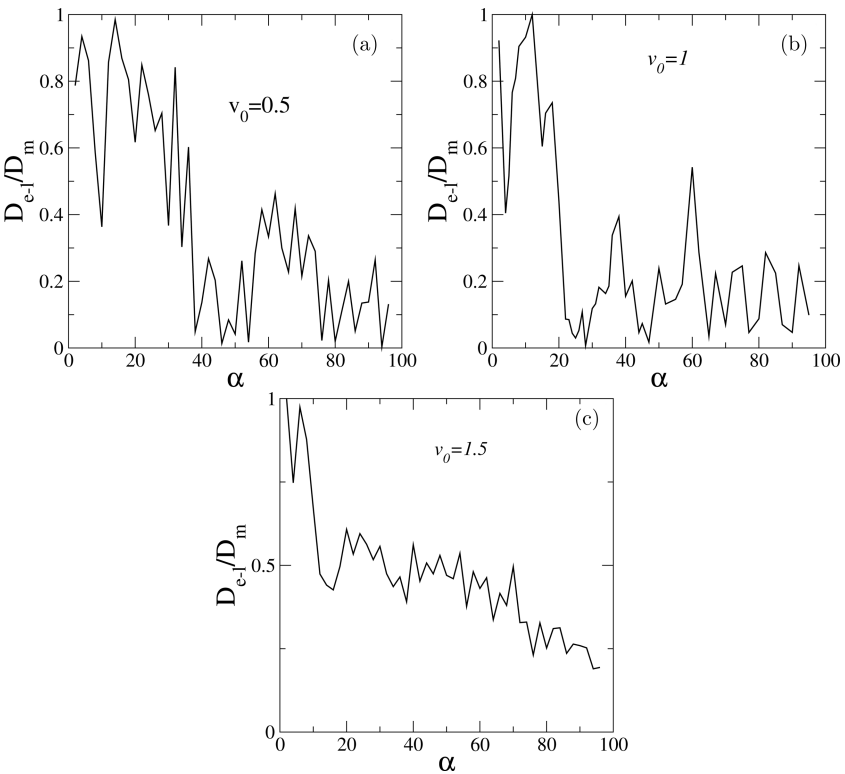

Fig. 3. Normalized distance between the electron and the lattice's deformation vs the electron–lattice interaction. The initial lattice velocity was $v_0 = 0.5$ upto 1.5.

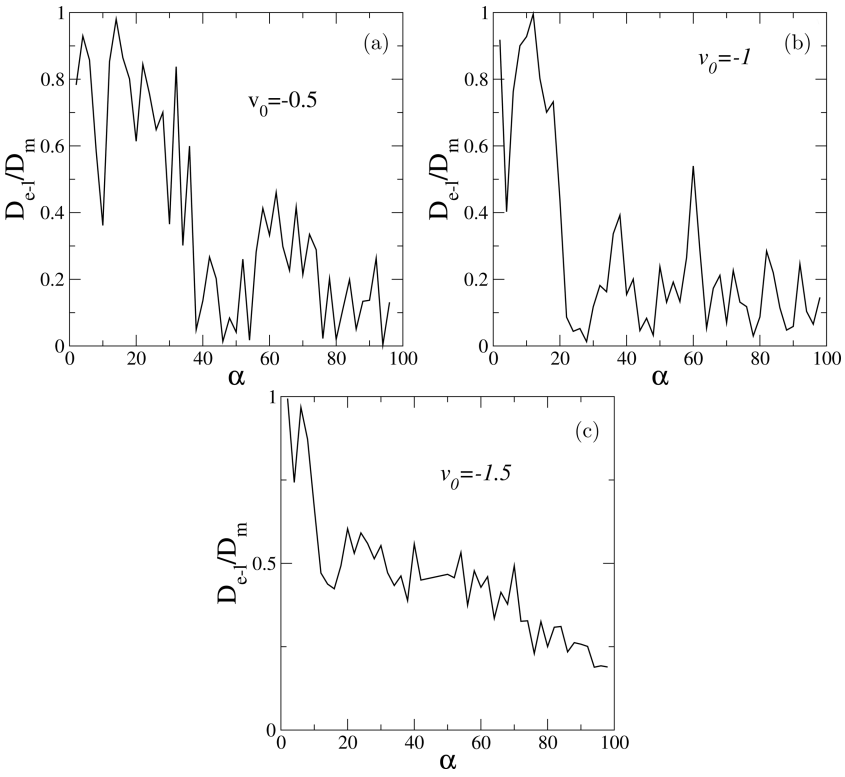

Fig. 4. Normalized distance between the electron and the lattice's deformation vs the electron–lattice interaction. The initial lattice velocity was $v_0 = -0.5$ upto -1.5.

calculations in these four previous pictures indeed suggest that the electron–lattice pair can exist only for some specific small intervals. For the most values of α, our results suggest that the electron wave function and the lattice deformation are kept separate. In Fig. 5, we show some details about the hopping distribution along the time and space for $\alpha = 5$ and $\alpha = 25$ (we considered $v_0 = 1$). We emphasize that in both cases ($\alpha = 5$ and 25) there is a solitonic mode with velocity roughly constant independent of α. For small α, the hopping distribution is about -1 in most parts of the chain, and, in a tiny region of the lattice, the hopping intensity shows a little growth. For $\alpha = 25$, we can observe again (see Fig. 5) a hopping profile in the plane t, n similar to that obtained for $\alpha = 5$. The difference now is the magnitude of the hopping peak (almost 10 times larger than the case with $\alpha = 5$). It is a direct consequence of the magnitude of the electron–lattice coupling. This region in which the hopping increases is exactly the position of solitonic deformation. Therefore, the solitonic deformation promotes the appearance of this hopping profile. This kind of "hopping wave" promotes the trapping of a finite fraction of the wave function. However, the amount of the wave function trapped by the "hopping profile" depends on the value of α and also v_0. In Fig. 6, we can see the fraction of the wave

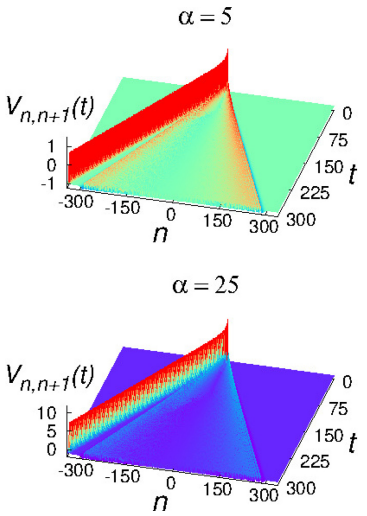

Fig. 5. The hopping parameter $V_{j,j+1}$ vs t and n for $\alpha = 5$ and $\alpha = 25$ (we considered $v_0 = 1$). We emphasize that the position $n = j - N/2 = 0$ here represents the center of chain.

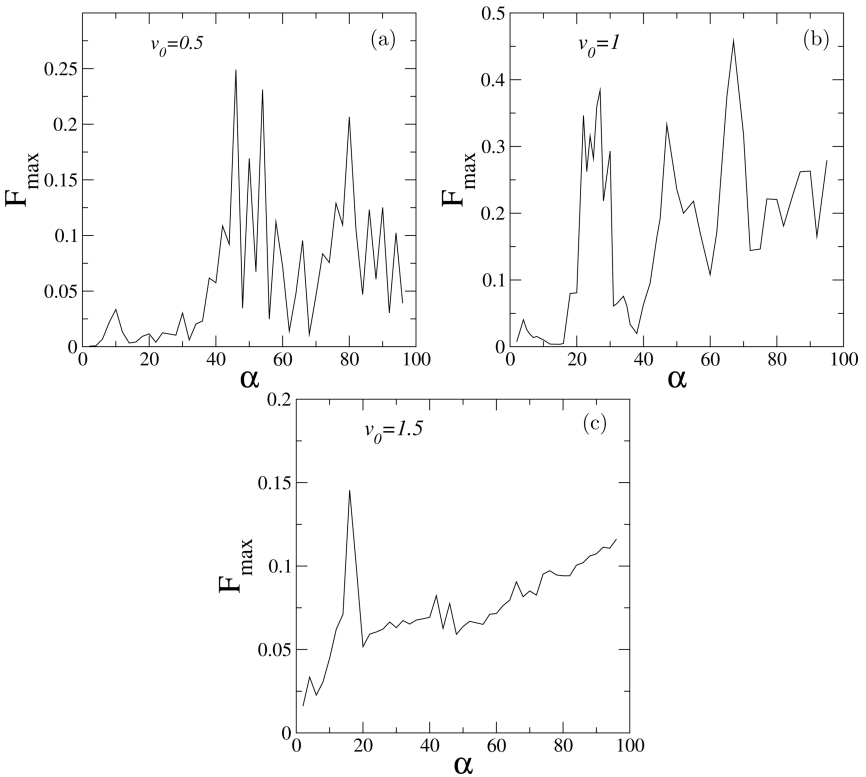

Fig. 6. The fraction of the wave function ($F_{\max} = [|c_j(t \approx t_m)|^2]_{\max}$) trapped by the solitonic lattice's deformation vs the electron–lattice interaction.

function ($F_{\max} = [|c_j(t \approx t_m)|^2]_{\max}$) vs the electron–lattice coupling α. We can see, for example, that, for $v_0 = 1$, the value of $F_{\max}(\alpha = 5)$ is much smaller than $F_{\max}(\alpha = 25)$. If you compare the figures of $F_{\max}$ for $v_0 = 0.5$ upto 1.5 we can see that the case with $v_0 = 1$ is the largest. For example, for $v_0 = 1$ and α within [24–30], we can see that the hopping profile can capture about 40% of the wave function. It is the key ingredient behind the results shown in Figs. 1 and 3. We emphasize that, for these parameters, we have obtained $V_e \approx V_L$ and the normalized distance $D_{e,L}/D_m$ almost zero. By another side, for $v_0 = 1$ and $\alpha \approx 10$ our calculations in Figs. 1 and 3 indicate that V_e and V_L are completely distinct and the normalized distance it was maximum. These results suggest a repulsion between the electron and the lattice's deformation. By analyzing the calculations for $F_{\max}$ for this case, we can see that the lattice's deformation was unable to trap a fraction of the wave function (i.e. $F_{\max}(\alpha = 10, v_0 = 1) \approx 0$). Therefore, based on Figs. 5 and 6, we can conclude that for $\alpha < 20$ the hopping distribution within the chain is, in general, unable to capture a dominant fraction of the electronic wave function. For $\alpha > 20$, depending on the value of v_0, it is possible to promote the electron–lattice pair formation. In general, for those intervals in which that $V_e \approx V_L$ and $D_{e,L}/D_m \to 0$, the fraction $F_{\max}$ of the electronic wave function captured by the lattice's deformation was pretty big. Our calculations reveal that when $V_e \approx V_L$ and $D_{e,L}/D_m \to 0$, the lattice's deformation trapped at least 30% of the initial wave-packet. Depending on the value of v_0 and α, about 50% of the electronic state was kept around the solitonic pulse.

Before concluding our work, we briefly discuss our calculations' dependence on the initial electronic condition. We will analyze the electron–soliton dynamics considering another initial one-electron state as, for example, $|\Phi(t = 0)\rangle = \sum_j c_j(t = 0)|j\rangle$ where $c_j(t = 0) = \delta_{j,N/2-50}$. Therefore, at the same instant $(t = 0)$ the classical lattice is excited using $Q_j(t = 0) = 0$ and $P_j = \delta_{j,N/2}$ and the electron is fully localized 50 sites distant from the center of the chain. Therefore, the electron will spread freely around the initial position for initial times while the solitonic mode propagates to the left side. To illustrate the electronic dynamics, we plot in Figs. 7(a) and 7(b), $|c_n|^2$ vs t and $n = j - N/2$. We emphasize that the position $n = j - N/2 = 0$ represents the center of the chain. In the absence of electron–soliton interaction ($\alpha = 0$), the electron wave packet will spread ballistically until the chain boundary (see Fig. 7(a)). In the presence of electron–soliton coupling ($\alpha = 1$), the electron initially spreads within the chain; however, after the solitonic mode meets the electron, the wave packet is swept away to the left side (see Fig. 7(b)). In Fig. 7(c), we can see the effect of the electron–soliton meeting on the electronic position along the time. For initial times, the electron centroid remains fixed at about -50 (the $n_e = 0$ represents the center of the chain; therefore, $n_e = -50$ is precisely the position we have initially localized the electron). For $t \approx 25$, the solitonic mode meets the electron and drags it to the left (see Fig. 7(c)). We can observe that, for $\alpha = 1$, the velocity of the lattice deformation and the electronic wave packet is roughly the same. We also observe in Fig. 7(d) that for $\alpha = 1$

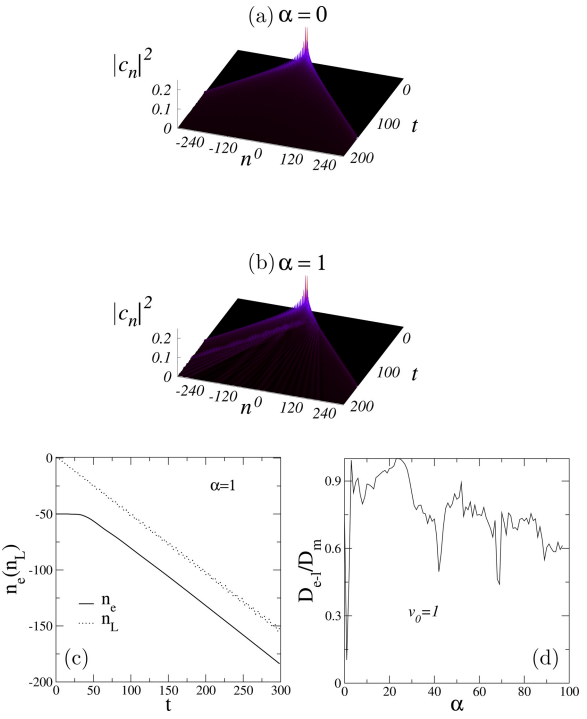

Fig. 7. Electron–soliton dynamics considering the initial one-electron state as $|\Phi(t=0)\rangle = \sum_j c_j(t=0)|j\rangle$ where $c_j(t=0) = \delta_{j,N/2-50}$. The classical lattice is excited using $Q_j(t=0) = 0$ and $P_j = \delta_{j,N/2}$. (a) $|c_n|^2$ vs t and $n = j - N/2$ for $\alpha = 0$. The electron wave packet will spread ballistically until the chain boundary. (b) The same in (a) for $\alpha = 1$; The electron initially spreads around the initial position; for time $t \approx 25$, the solitonic mode meets the electron, and most part of the electronic wave packet is pushed to the left side. (c) The electron and the lattice position vs time for $\alpha = 1$. (d) Normalized distance between the electron and the lattice's deformation vs the electron–lattice interaction.

the normalized distance between soliton and electron is small, thus suggesting the existence of an electron–soliton pair. Therefore, for this new initial condition, our results are qualitatively similar. Whenever the solitonic excitation meets a wide (or broad) electronic wave packet, it is still possible to establish an electron–solitonic excitation and effectively control the electron propagation.

4. Summary and Final Statement

We investigate the problem of electronic dynamics in a chain with cubic nonlinearity. We solved the Schrödinger equation by using a Taylor procedure. We used Verlet velocity formalism to solve the lattice's dynamics. Using this numerical formalism, we describe the electron–lattice pair formation and its particularities in detail. Here we investigate the possibility of the electron–lattice pair and its dependence on the initial lattice's velocity and the electron–lattice coupling. Our results indicate the necessary condition to promote the electron–soliton dynamics. We discuss the

fraction of the electronic wave function captured by the lattice's deformations. We investigate the electronic hopping vs time and chain position. We have shown that for strong electron–lattice interaction, the hopping profile exhibits an intense peak that facilitates the electron controls. Our results demonstrate that the electron–soliton pairs occur for some specific values of α and v_0. Therefore, our calculations indicate that the phenomenology of electron–soliton propagation is a rare effect. To obtain a cooperative dynamics profile evolving the electron and solitonic pulse close with the same velocity, we need to adjust v_0 and α within specific small intervals. We hope our work stimulates further investigation of electron–soliton dynamics in solid-state systems.

Acknowledgments

This work is supported by CNPq, CAPES and FINEP (Federal Brazilian Agencies) and FAPEAL (Alagoas State Agency).

References

1. G. Xing, Y. Miura and T. Tadano, *Phys. Rev. B* **105**, 104427 (2022).
2. P. Kurzhals *et al.*, *Nat. Commun.* **13**, 228 (2022).
3. R. P. Chatelain, V. R. Morrison, B. L. M. Klarenaar and B. J. Siwick, *Phys. Rev. Lett.* **113**, 235502 (2014).
4. T. Konstantinova *et al.*, *Sci. Adv.* **4**, eaap7427 (2018).
5. D. Zahn, H. Seiler, Y. W. Windsor and R. Ernstorfer, *Struct. Dyn.* **8**, 064301 (2021).
6. A. P. Chetverikov, W. Ebeling, E. del Rio, K. S. Sergeev and M. G. Velarde, *Chaos Solitons Fractals* **150**, 111179 (2021).
7. I. A. Shepelev, S. V. Dmitriev, A. A. Kudreyko, M. G. Velarde and E. A. Korznikova, *Chaos Solitons Fractals* **140**, 110217 (2020).
8. W. P. Su, J. R. Schrieffer and A. J. Heeger, *Phys. Rev. Lett.* **42**, 1698 (1979); *Phys. Rev. B* **22**, 2099 (1980); A. J. Heeger, S. Kivelson, J. R. Schrieffer and W.-P. Su, *Rev. Mod. Phys.* **60**, 781 (1988).
9. E. Meier, F. An and B. Gadway, *Nat. Commun.* **7**, 13986 (2016).
10. C. Skokos, D. O. Krimer, S. Komineas and S. Flach, *Phys. Rev. E* **79**, 056211 (2009); **89**, 029907 (2014).
11. D. Leykam, S. Flach, O. Bahat-Treidel and A. S. Desyatnikov, *Phys. Rev. B* **88**, 224203 (2013); G. Gligorić, K. Rayanov and S. Flach, *Europhys. Lett.* **101**, 10011 (2013).
12. T. V. Laptyeva, J. D. Bodyfelt and S. Flach, *Europhys. Lett.* **98**, 60002 (2012); M. Larcher, T. V. Laptyeva, J. D. Bodyfelt, F. Dalfovo, M. Modugno and S. Flach, *New J. Phys.* **14**, 103036 (2012).
13. C. Skokos and S. Flach, *Phys. Rev. E* **82**, 016208 (2010).
14. M. V. Ivanchenko, T. V. Laptyeva and S. Flach, *Phys. Rev. Lett.* **107**, 240602 (2011).
15. C. Skokos, I. Gkolias and S. Flach, *Phys. Rev. Lett.* **111**, 064101 (2013).
16. J. D. Bodyfelt, T. V. Laptyeva, G. Gligoric, D. O. Krimer, C. Skokos and S. Flach, *Int. J. Bifurcation Chaos* **21**, 2107 (2011).
17. S. Flach, *Springer Proc. Phys.* **173**, 45 (2016).
18. T. V. Laptyeva, M. V. Ivanchenko and S. Flach, *J. Phys. A* **47**, 493001 (2014).
19. A. Pikovsky, *J. Stat. Mech., Theory Exp.* **2015**, P08007 (2015).

20. F. A. B. F. de Moura, I. Gléria, I. F. dos Santos and M. L. Lyra, *Phys. Rev. Lett.* **103**, 096401 (2009).
21. Z. Pan, S. Xiong and C. Gong, *Phys. Rev. E* **56**, 4744 (1997); H. Yamada and K. Iguchi, *Adv. Condens. Matter Phys.* **2010**, 380710 (2010).
22. G. Kopidakis, S. Komineas, S. Flach and S. Aubry, *Phys. Rev. Lett.* **100**, 084103 (2008); A. S. Pikovsky and D. L. Shepelyansky, *Phys. Rev. Lett.* **100**, 094101 (2008); D. Hajnal and R. Schilling, *Phys. Rev. Lett.* **101**, 124101 (2008).
23. Y. Lahini, A. Avidan, F. Pozzi, M. Sorel, R. Morandotti, D. N. Christodoulides and Y. Silberberg, *Phys. Rev. Lett.* **100**, 013906 (2008).
24. J.-K. Xue and A.-X. Zhang, *Phys. Rev. Lett.* **101**, 180401 (2008); N. Akhmediev, A. Ankiewicz and J. M. Soto-Crespo, *Phys. Rev. E* **80**, 026601 (2009); S. A. Ponomarenko and G. P. Agrawal, *Phys. Rev. Lett.* **97**, 013901 (2006); A. Maluckov, L. Hadzievski, N. Lazarides and G. P. Tsironis, *Phys. Rev. E* **79**, 025601(R) (2009); T. Anker, M. Albiez, R. Gati, S. Hunsmann, B. Eiermann, A. Trombettoni and M. K. Oberthaler, *Phys. Rev. Lett.* **94**, 020403 (2005).
25. Z. Pan, S. Xiong and C. Gong, *Phys. Rev. B* **56**, 1063 (1997).
26. J. E. Macías-Díaz and I. E. Medina-Ramírez, *Commun. Nonlinear Sci. Numer. Simul.* **14**, 3200 (2009).
27. N. J. Zabusky, *Chaos* **15**, 015102 (2005).
28. T. Dauxois, M. Peyrard and S. Ruffo, *Eur. J. Phys.* **26**, S3 (2005).
29. L. Brizhik, A. P. Chetverikov, W. Ebeling, G. Ropke and M. G. Velarde, *Phys. Rev. B* **85**, 245105 (2012).
30. A. P. Chetverikov, W. Ebeling and M. G. Velarde, *Phys. D* **240**, 1954 (2011).
31. D. Hennig, M. G. Velarde, W. Ebeling and A. Chetverikov, *Phys. Rev. E* **78**, 066606 (2008).
32. D. Hennig, A. Chetverikov, M. G. Velarde and W. Ebeling, *Phys. Rev. E* **76**, 046602 (2007).
33. V. A. Makarov, M. G. Velarde, A. P. Chetverikov and W. Ebeling, *Phys. Rev. E* **73**, 066626 (2006).
34. D. Hennig, C. Neissner, M. G. Velarde and W. Ebeling, *Phys. Rev. B* **73**, 024306 (2006).
35. A. S. Davydov, *Solitons in Molecular Systems*, 2nd edn. (Reidel, Dordrecht, 1991).
36. A. C. Scott, *Phys. Rep.* **217**, 1 (1992).
37. A. S. Davydov, *Phys. Scr.* **20**, 387 (1979).
38. A. S. Davydov, *J. Theor. Biol.* **66**, 379 (1977).
39. A. S. Davydov, *Biology and Quantum Mechanics* (Pergamon, New York, 1982).
40. B. J. Alder, K. J. Runge and R. T. Scalettar, *Phys. Rev. Lett.* **79**, 3022 (1997).
41. L. S. Brizhik and A. A. Eremko, *Phys. D* **81**, 295 (1995).
42. O. G. Cantu Ross, L. Cruzeiro, M. G. Velarde and W. Ebeling, *Eur. Phys. J. B* **80**, 545 (2011).
43. M. G. Velarde and C. Neissner, *Int. J. Bifurcation Chaos* **18**, 885 (2008).
44. M. G. Velarde, W. Ebeling and A. P. Chetverikov, *Int. J. Bifurcation Chaos* **21**, 1595 (2011).
45. A. P. Chetverikov, W. Ebeling and M. G. Velarde, *Eur. Phys. J. B* **80**, 137 (2011).
46. M. G. Velarde, W. Ebeling and A. P. Chetverikov, *Int. J. Bifurcation Chaos* **15**, 245 (2005).
47. M. G. Velarde, *J. Comput. Appl. Math.* **233**, 1432 (2010).
48. M. G. Velarde, W. Ebeling and A. P. Chetverikov, *Eur. Phys. J. B* **85**, 291 (2012).
49. W. Ebeling, A. P. Chetverikov, G. Röpke and M. G. Velarde, *Contrib. Plasma Phys.* **53**, 736 (2013).

50. A. P. Chetverikov, W. Ebeling and M. G. Velarde, *Eur. Phys. J., Spec. Top.* **222**, 2531 (2013).
51. M. G. Velarde, A. P. Chetverikov, W. Ebeling, E. G. Wilson and K. J. Donovan, *Europhys. Lett.* **106**, 27004 (2014).
52. A. P. Chetverikov, W. Ebeling, V. D. Lakhno and M. G. Velarde, *Phys. Rev. E* **100**, 052203 (2019).
53. M. O. Sales and F. A. B. F. de Moura, *J. Phys., Condens. Matter* **26**, 415401 (2014).
54. J. L. L. dos Santos, M. O. Sales, A. Ranciaro Neto and F. A. B. F. de Moura, *Phys. Rev. E* **95**, 052217 (2017).
55. M. Kataoka, M. R. Astley, A. L. Thorn, C. H. W. Barnes, C. J. B. Ford, D. Anderson, G. A. C. Jones, I. Farrer, D. A. Ritchie and M. Pepper, *Phys. E, Low-Dimens. Syst. Nanostruct.* **40**, 1017 (2008).
56. M. Kataoka, M. R. Astley, A. L. Thorn, D. K. L. Oi, C. H. W. Barnes, C. J. B. Ford, D. Anderson, G. A. C. Jones, I. Farrer, D. A. Ritchie and M. Pepper, *Phys. Rev. Lett.* **102**, 156801 (2009).
57. J.-H. He, J. Gao and H.-Z. Guo, *Appl. Phys. Lett.* **97**, 122107 (2010).
58. S. Hermelin, S. Takada, M. Yamamoto, S. Tarucha, A. D. Wieck, L. Saminadayar, C. Bäuerle and T. Meunier, *Nature* **477**, 435 (2011).
59. R. P. G. McNeil, M. Kataoka, C. J. B. Ford, C. H. W. Barnes, D. Anderson, G. A. C. Jones, I. Farrer and D. A. Ritchie, *Nature* **477**, 439 (2011).
60. V. Miseikis, J. E. Cunningham, K. Saeed, R. O'Rorke and A. G. Davies, *Appl. Phys. Lett.* **100**, 133105 (2012).
61. S. Takada *et al.*, *Nat. Commun.* **10**, 4557 (2019).
62. T.-K. Hsiao *et al.*, *Nat. Commun.* **11**, 917 (2020).
63. R. Ito, S. Takada, A. Ludwig, A. D. Wieck, S. Tarucha and M. Yamamoto, *Phys. Rev. Lett.* **126**, 070501 (2021).
64. Y. Zhou, N. Zhang, D. J. Bisharat, R. J. Davis, Z. Zhang, J. Friend, P. R. Bandaru and D. F. Sievenpiper, arXiv:2111.12249.
65. M. P. Alan and D. J. Tildesley, *Computer Simulation of Liquids* (Oxford University Press, 1987), pp. 71–80.
66. F. A. B. F. de Moura, *Int. J. Mod. Phys. C* **22**, 63 (2011).